

Supplementary material

Sub-Saharan Africa sweetpotato virome

Ricardo I. ALCALÁ-BRISEÑO

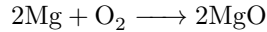
June 2, 2021

Abstract

Results and supplementary figures of the Sub-Saharan Africa sweetpotato virome (SSA-SPV).

1 Gravity model

We evaluate the cropland density of sweetpotato using a cropland connectivity risk index (Yanru et al., 2020). Implementing a gravity model using a negative exponential distribution using the sweetpotato density of 1degree pixel from the Monfreda and MapSpam databases (REFs). We calculated the distance between land crop densities as land unit pixels (LUPs) of sweetpotato using a gravity model described by Xing, et al. We aggregated the mean harvested area of two popular datasets of global cropland area for Sub-Saharan Africa into maps with 2 degrees resolution (120 x 120 minutes). The likelihood of movement between two LUPs was evaluated using a negative exponential function of the distance between the two, $\exp(-\gamma d_{ij})$, using ten values of γ (0.05, 0.1, 0.2, 0.3, to 1) in a sensitivity analysis, where higher values represent a lower likelihood of pathogen or vector movement between sweetpotato LUPs. We evaluated distances across sweetpotato production in Sub-Saharan Africa, evaluating the LUPs corresponding to the virome samples clustered into sweetpotato regions identified using unsupervised machine learning, specifically a k-means clustering algorithm. Twenty k-clusters were tested with gap-statistics (Monte Carlo bootstraps of 10,000 replicates and 100 iterations), yielding the same seven k-clusters for negative exponential parameter γ in the range of 0.3 to 1. The seven sweetpotato regions, used in individual network analyses, were 1) Tanzania and Uganda; 2) Guinea; 3) Benin, Ghana, and Nigeria; 4) Malawi, Mozambique, Tanzania, and Zimbabwe; 5) Mozambique and Zimbabwe; 6) Ethiopia and 7) Angola (Table 1).



1.1 Regions

Seven regions of sweetpotato were identified with a gravity model (table 1).

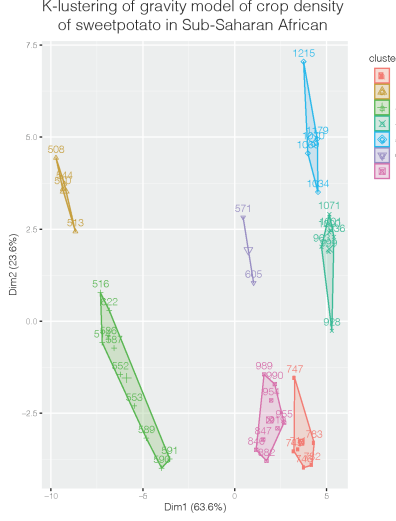


Figure 1: Gravity model Sub-Saharan Africa sweetpotato virome.

K-cluster	Regions	Countries	Samples
Region 1	East	Tanzania, Uganda	228
Region 2	Near West	Ghana, Benin and Nigeria	36
Region 3	Southwest	Angola	171
Region 4	East group 1	Mozambique, Zimbabwe	262
Region 5	East group 2	Mozambique, Tanzania, Zimbabwe	151
Region 6	East group 3	Rwanda, Tanzania, Uganda	261
Region 7	Far East	Ethiopia	171
Total			1286

2 Regions

2.1 Region 1

Region 1 corresponding to East Africa (Tanzania and Uganda) of 228 samples collected. We identified 98 viruses species, in ----- genera, and ----- families. A barplot representing the frequency distribution and relative abundance of SSA-SPV region 1 (Fig. 2)

2.2 Region 2

Region 1 corresponding to near Weast Africa (Ghana, Benin and Nigeria) of 36 samples collected. We identified 55 viruses species, in ----- genera, and ----- families. A barplot representing the frequency distribution and relative

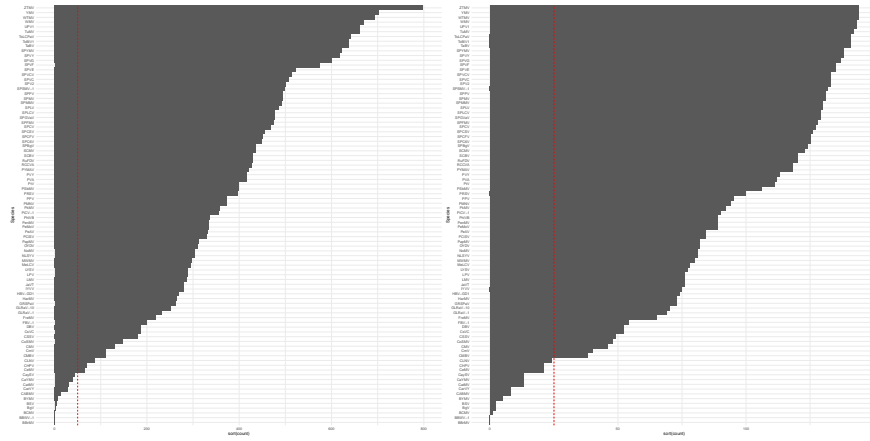


Figure 2: Incidence distribution Sub-Saharan Africa sweetpotato virome region 1.

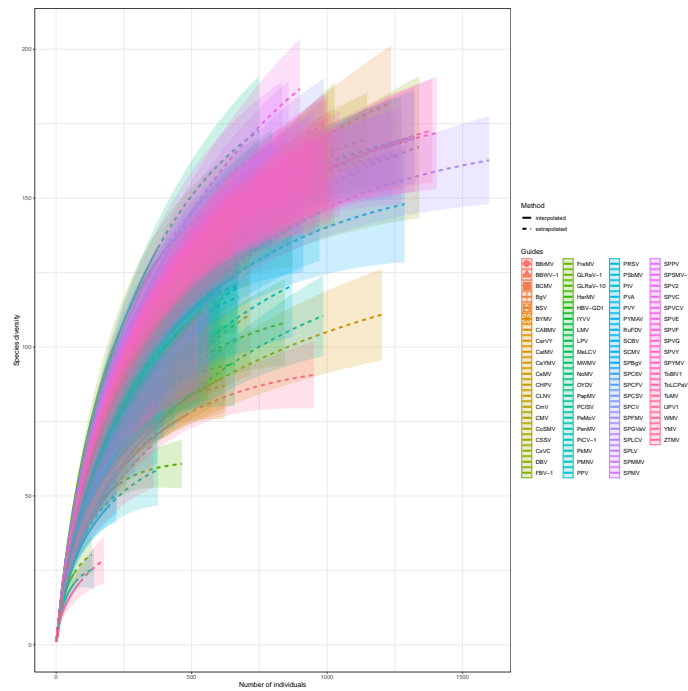


Figure 3: Rarefaction of Sub-Saharan Africa sweetpotato virome region 1.

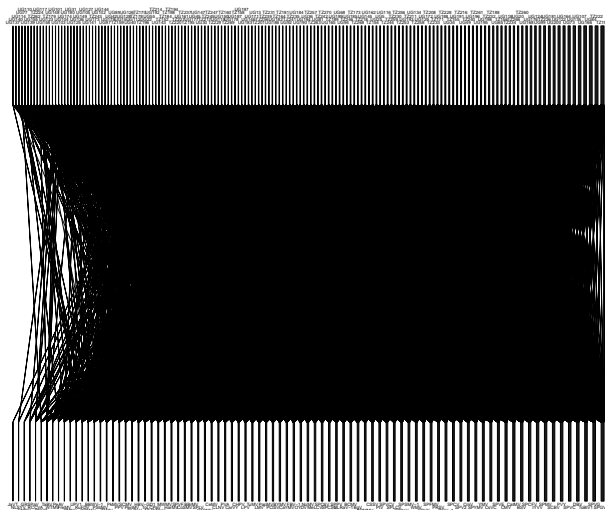


Figure 4: Bipartite network Sub-Saharan Africa sweetpotato virome region 1.

abundance of SSA-SPV region 1 (Fig. 6)

2.3 Region 3

2.4 Region 4

2.5 Region 5

2.6 Region 6

2.7 Region 7

3 Networks metrics

Mass of magnesium metal	= 8.59 g - 7.28 g
	= 1.31 g
Mass of magnesium oxide	= 9.46 g - 7.28 g
	= 2.18 g
Mass of oxygen	= 2.18 g - 1.31 g
	= 0.87 g

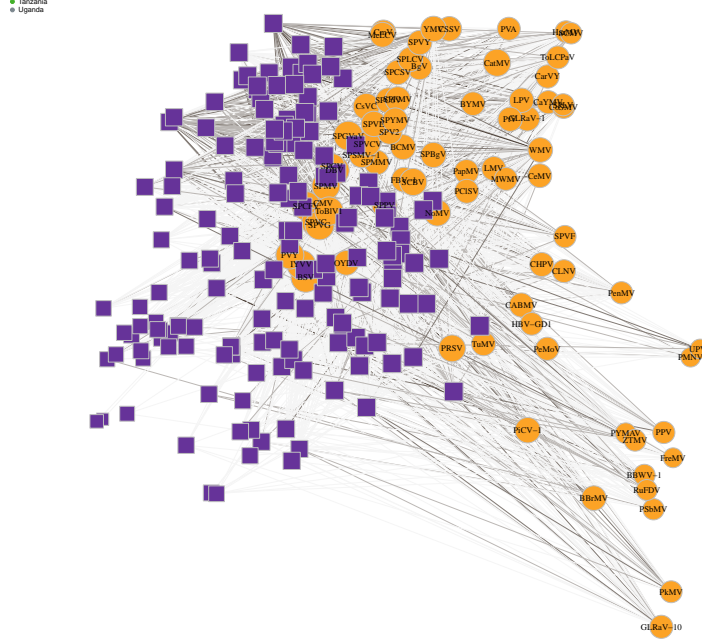


Figure 5: Bipartite network Sub-Saharan Africa sweetpotato virome region 1, Kimura-Kawai layout

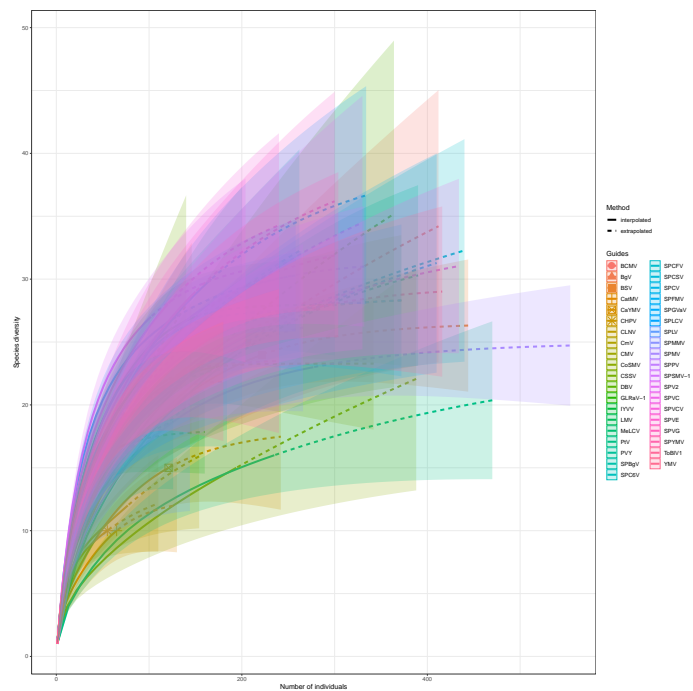
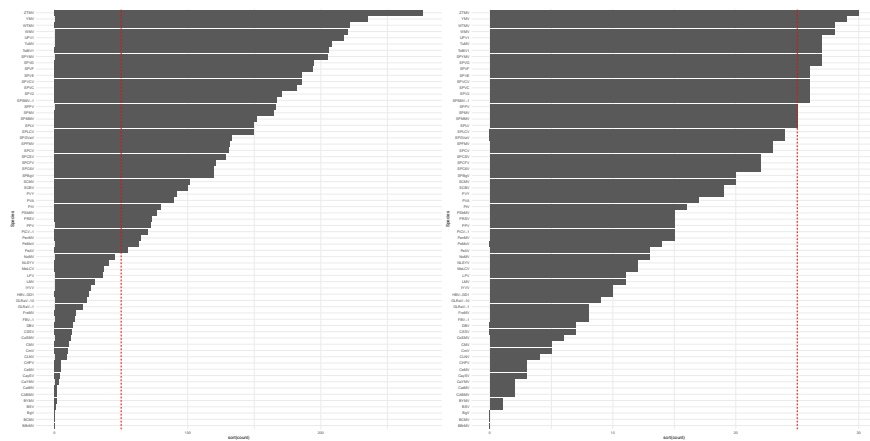
Because of this reaction, the required ratio is the atomic weight of magnesium: 16.00 g of oxygen as experimental mass of Mg: experimental mass of oxygen or $\frac{x}{1.31} = \frac{16}{0.87}$ from which, $M_{\text{Mg}} = 16.00 \times \frac{1.31}{0.87} = 24.1 = 24 \text{ g mol}^{-1}$ (to two significant figures).

4 Results and Conclusions

The atomic weight of magnesium is concluded to be 24 g mol^{-1} , as determined by the stoichiometry of its chemical combination with oxygen. This result is in agreement with the accepted value.

5 Discussion of Experimental Uncertainty

The accepted value (periodic table) is 24.3 g mol^{-1} Smith and Jones (2012). The percentage discrepancy between the accepted value and the result obtained



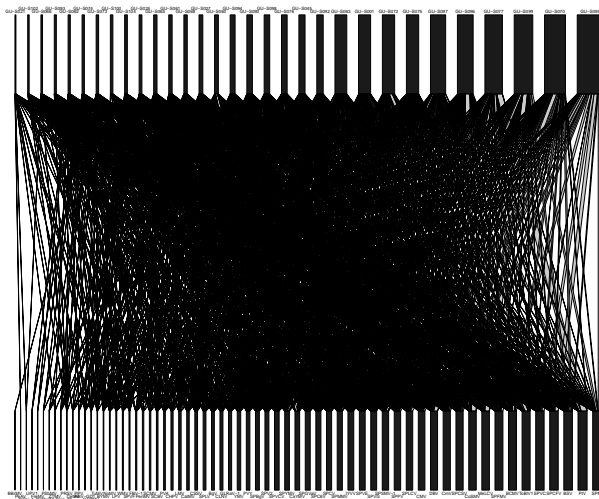


Figure 8: Bipartite network Sub-Saharan Africa sweetpotato virome region 1.

here is 1.3%. Because only a single measurement was made, it is not possible to calculate an estimated standard deviation.

The most obvious source of experimental uncertainty is the limited precision of the balance. Other potential sources of experimental uncertainty are: the reaction might not be complete; if not enough time was allowed for total oxidation, less than complete oxidation of the magnesium might have, in part, reacted with nitrogen in the air (incorrect reaction); the magnesium oxide might have absorbed water from the air, and thus weigh “too much.” Because the result obtained is close to the accepted value it is possible that some of these experimental uncertainties have fortuitously cancelled one another.

6 Answers to Definitions

- a. The *atomic weight of an element* is the relative weight of one of its atoms compared to C-12 with a weight of 12.0000000. . . , hydrogen with a weight of 1.008, to oxygen with a weight of 16.00. Atomic weight is also the average weight of all the atoms of that element as they occur in nature.
- b. The *units of atomic weight* are two-fold, with an identical numerical value.

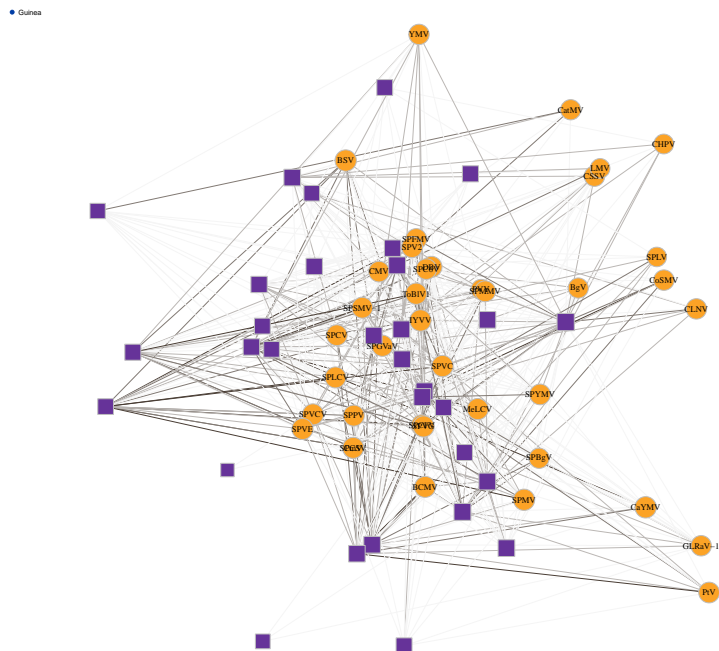


Figure 9: Bipartite network Sub-Saharan Africa sweetpotato virome region 1, Kimura-Kawai layout

They are g/mole of atoms (or just g/mol) or amu/atom.

- c. *Percentage discrepancy* between an accepted (literature) value and an experimental value is

$$\frac{\text{experimental result} - \text{accepted result}}{\text{accepted result}}$$

References

Smith, J. M. and Jones, A. B. (2012). *Chemistry*. Publisher, 7th edition.

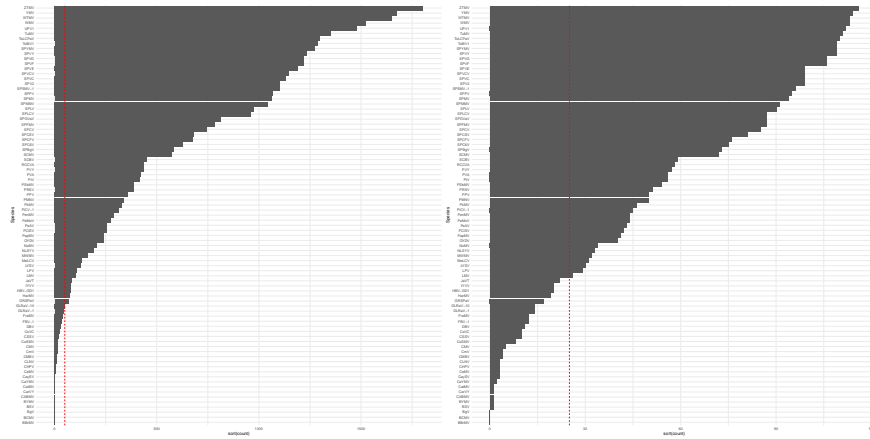


Figure 10: Incidence distribution Sub-Saharan Africa sweetpotato virome region 1.

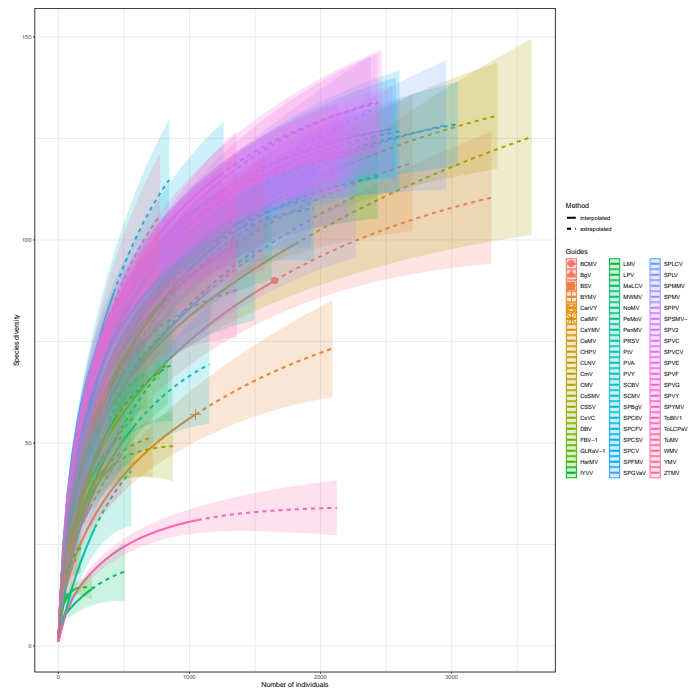


Figure 11: Rarefaction of Sub-Saharan Africa sweetpotato virome region 1.

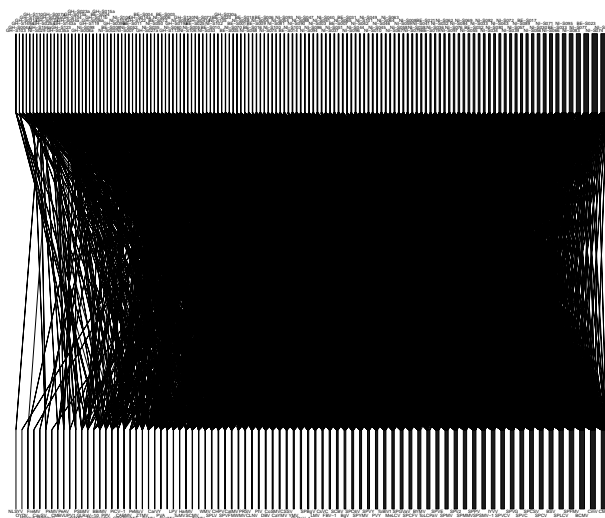


Figure 12: Bipartite network Sub-Saharan Africa sweetpotato virome region 1.

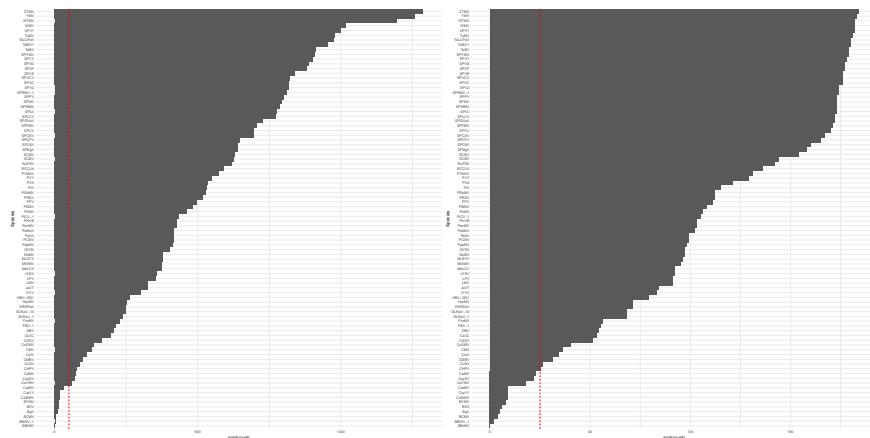


Figure 14: Incidence distribution Sub-Saharan Africa sweetpotato virome region 1.

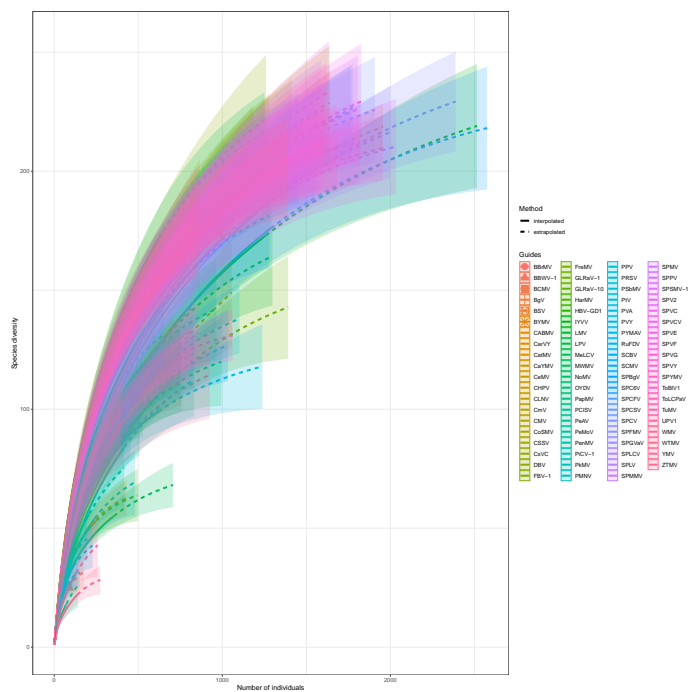


Figure 15: Rarefaction of Sub-Saharan Africa sweetpotato virome region 1.

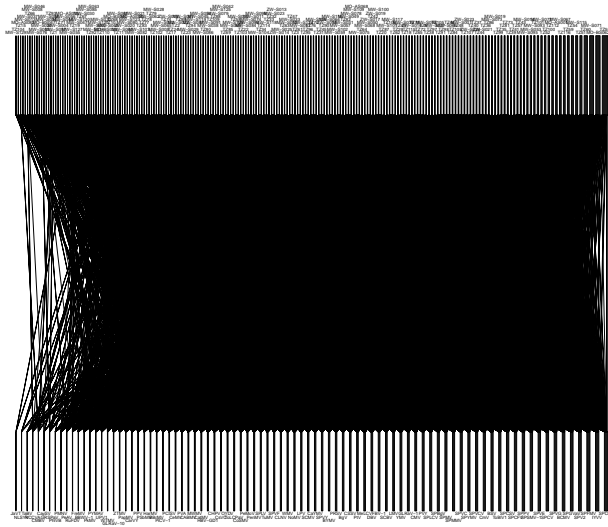


Figure 16: Bipartite network Sub-Saharan Africa sweetpotato virome region 1.

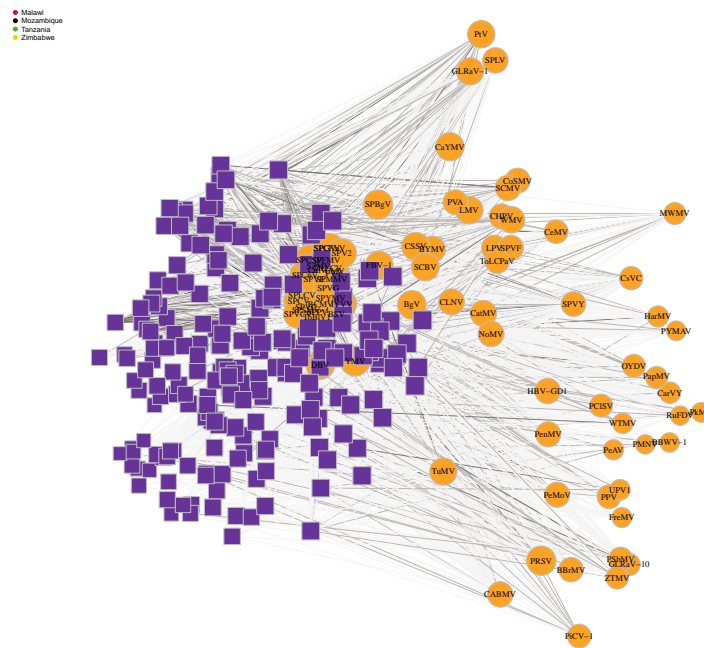
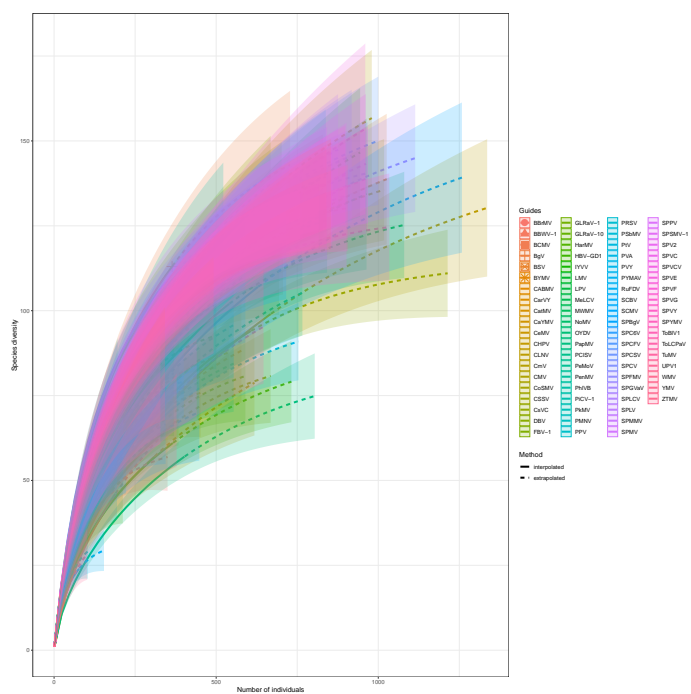
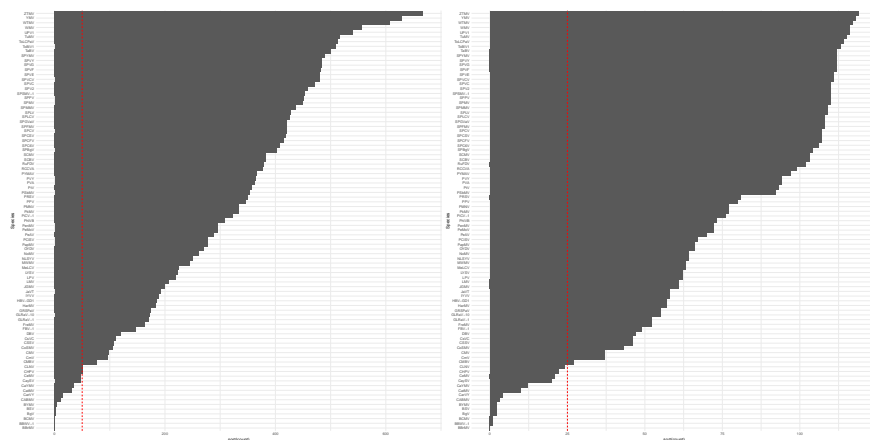


Figure 17: Bipartite network Sub-Saharan Africa sweetpotato virome region 1, Kimura-Kawai layout



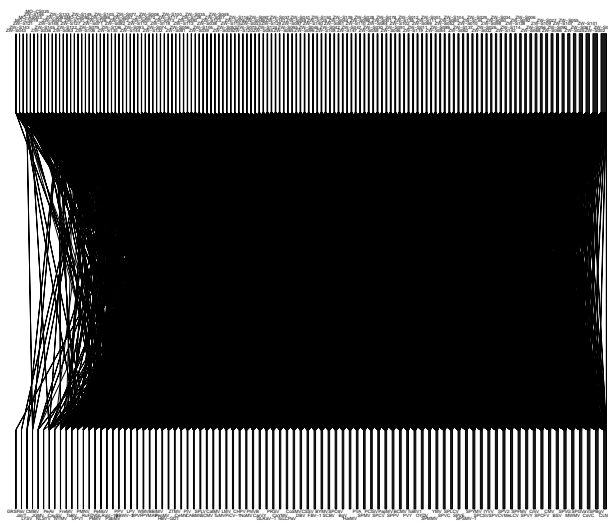


Figure 20: Bipartite network Sub-Saharan Africa sweetpotato virome region 1.

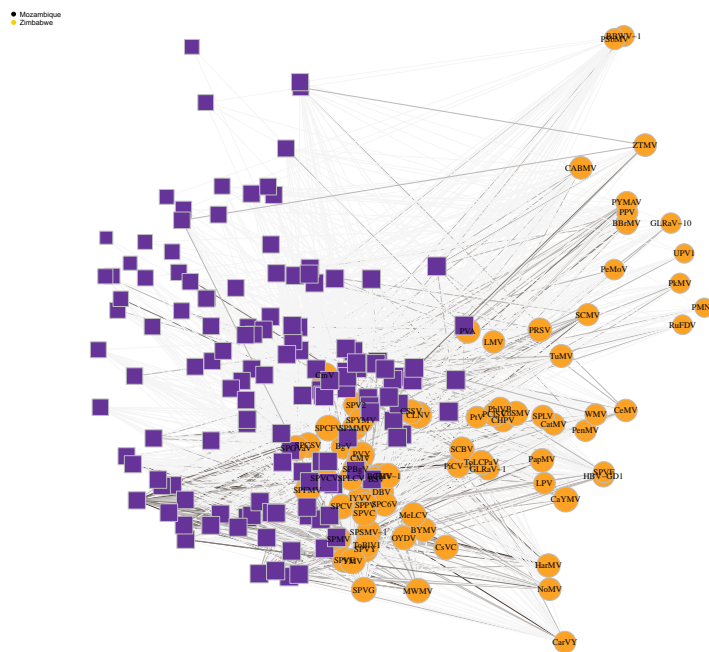
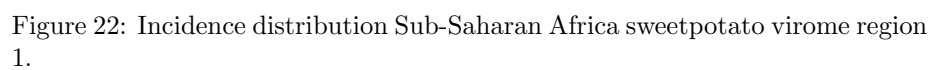


Figure 21: Bipartite network Sub-Saharan Africa sweetpotato virome region 1, Kimura-Kawai layout



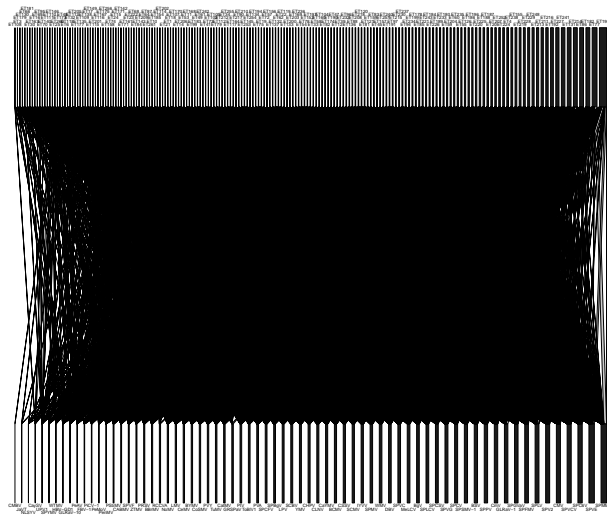


Figure 24: Bipartite network Sub-Saharan Africa sweetpotato virome region 1.

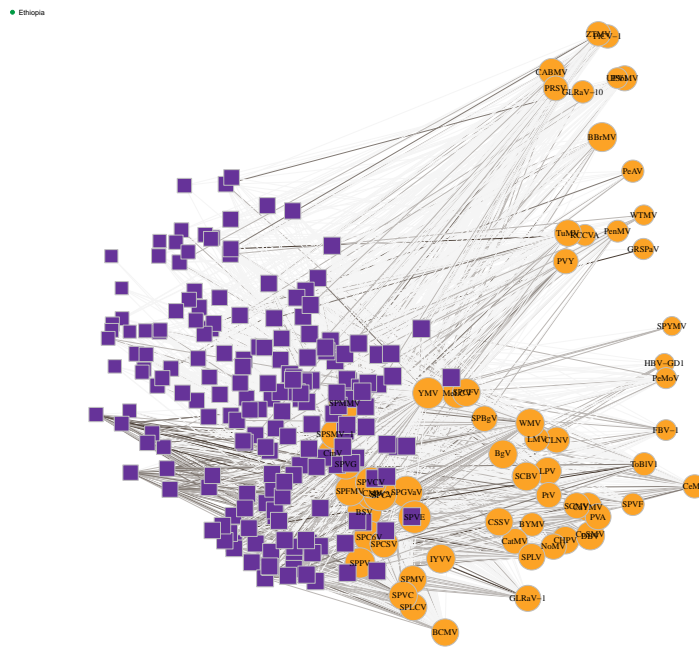


Figure 25: Bipartite network Sub-Saharan Africa sweetpotato virome region 1, Kimura-Kawai layout

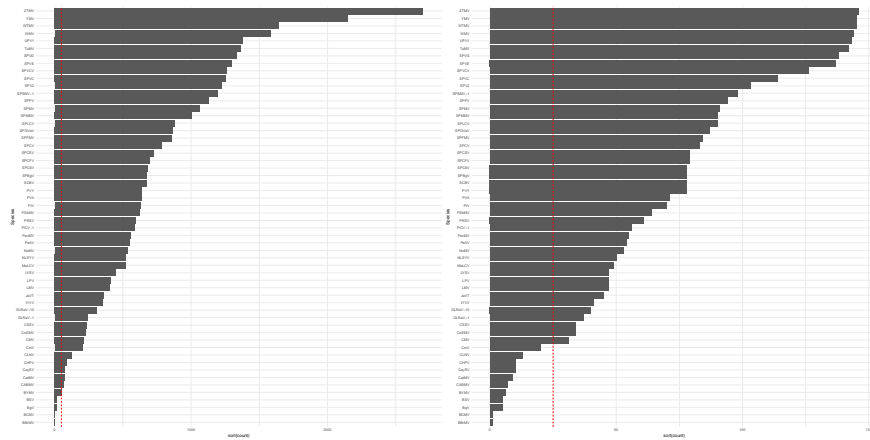


Figure 26: Incidence distribution Sub-Saharan Africa sweetpotato virome region 1.

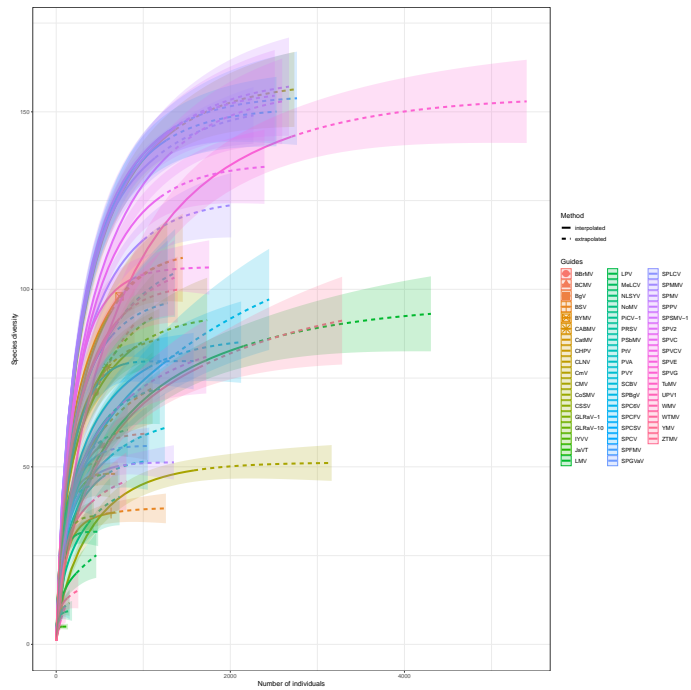


Figure 27: Rarefaction of Sub-Saharan Africa sweetpotato virome region 1.

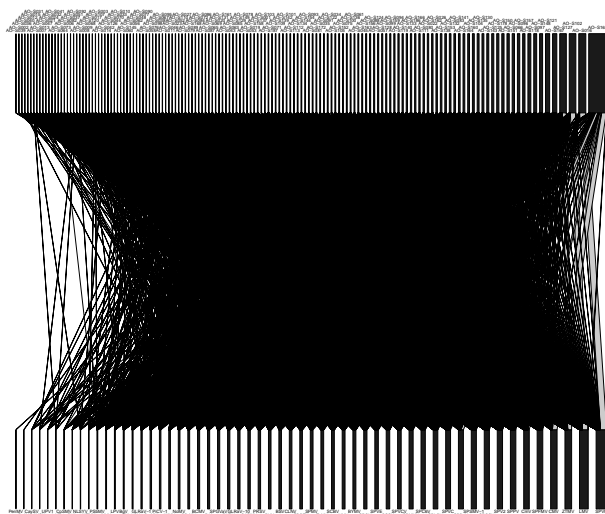


Figure 28: Bipartite network Sub-Saharan Africa sweetpotato virome region 1.

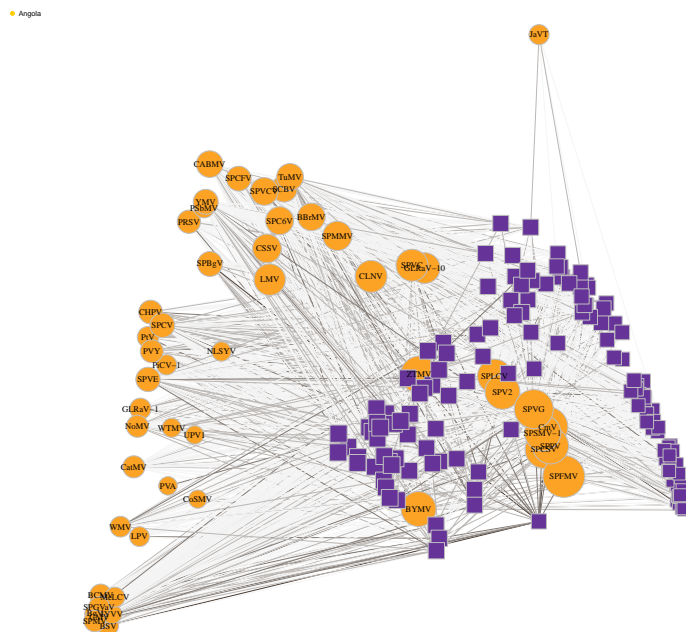


Figure 29: Bipartite network Sub-Saharan Africa sweetpotato virome region 1, Kimura-Kawai layout

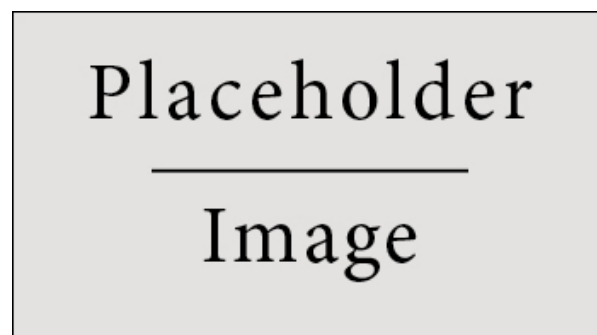


Figure 30: Figure caption.